

Cite this: *New J. Chem.*, 2011, **35**, 1004–1010

www.rsc.org/njc

PAPER

A binaphthol-substituted tetrathiafulvalene with axial chirality and its enantiopure TCNQF₄ charge-transfer salts†

Ali Saad, Olivier Jeannin and Marc Fourmigué*

Received (in Montpellier, France) 18th January 2011, Accepted 15th February 2011

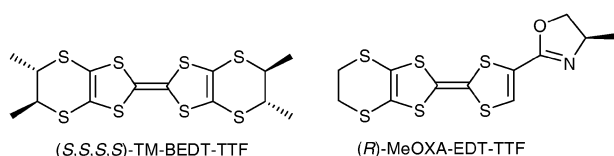
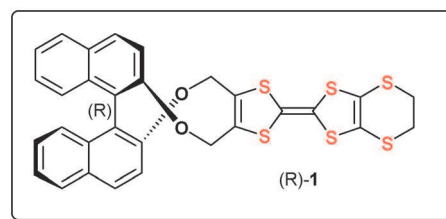
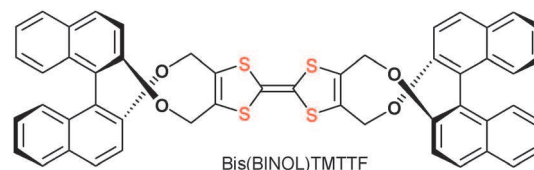
DOI: 10.1039/c1nj20034h

A chiral tetrathiafulvalene (**1**) bearing a binaphtholdimethylene moiety on one side, an ethylenedithio substituent on the other side, is prepared from atropisomeric (*R*)-, (*S*)- and racemic (*R,S*)-binaphthol. Its oxidation potential (0.49 V vs. SCE) allows for its oxidation with TCNQF₄. Crystal structures of the neutral racemic (*R,S*)-**1** and enantiopure (*R*)-**1** were determined together with those of the enantiopure charge-transfer salts formulated as [(*R*)-**1**][TCNQF₄].CH₂Cl₂ and [(*S*)-**1**][TCNQF₄].CH₂Cl₂, the first enantiomeric salts of chiral TTFs with axial chirality. Despite the peculiar geometry adopted by the binaphthyl moieties in the constrained ten-membered ring in **1**, stacking of the donor molecules is observed, both in the neutral state and in the TCNQF₄ charge transfer salts where the (**1**)^{•+} and (TCNQF₄)^{•−} radical species are associated, respectively, into [(**1**)₂]²⁺ and [(TCNQF₄)₂]^{2−} homodyads, both in their singlet state.

Introduction

In the search for hybrid organic conductors associating, eventually in a synergistic way, two different properties,¹ the combination of metallic conductivity with chirality has recently raised a strong interest,^{2,3} based on the expected observation of the so-called electrical magneto-chiral anisotropy effect.⁴ For tetrathiafulvalene-based (TTF) cation radical salts, chirality can be introduced, either on the counter anion,^{5,6} on an embedded chiral solvent molecule,⁷ or on the donor molecule. Taking advantage of the flexibility offered by organic chemistry of chiral species and availability of molecules from chiral pool, different series of chiral tetrathiafulvalenes have been already synthesised, from the initial (S,S,S,S)-tetramethyl BEDT-TTF⁸ and analogs^{9,10} to more recent oxazoline derivatives such as MeOXA-EDT-TTF.¹¹ Only a few of all these donor molecules were successfully engaged in a variety of chiral cation radical salts,^{10–13} and in most cases, the partially oxidized conducting stacks or slabs adopt a pseudo-centrosymmetric structure and the chiral centre does not play a crucial role in the solid state organisation.

In order to induce stronger chiral effects in the solid state, we considered the introduction of axial chirality such as that found in atropisomers of binaphthol derivatives, since binaphthol itself is easily available, as a racemic mixture and in the two enantiomeric forms. Highly flexible binaphthol derivatives bearing two TTF moieties have been reported recently by Martin *et al.*¹⁴ and Zhu *et al.*¹⁵ with the aim of controlling their circular dichroism response through electron transfer processes. Our approach toward more rigid molecules led us recently to report the preparation of the symmetrical bis-(BINOL)TMTTF molecule, as the diastereomeric mixture, or as pure (*R,R*), (*S,S*) or *meso* forms.¹⁶



Sciences Chimiques de Rennes, Université Rennes 1,
UMR CNRS 6226, Campus de Beaulieu, 35042 Rennes, France.
E-mail: marc.fourmigue@univ-rennes1.fr

† CCDC reference numbers 809759–809762. For crystallographic data in CIF or other electronic format see DOI: 10.1039/c1nj20034h

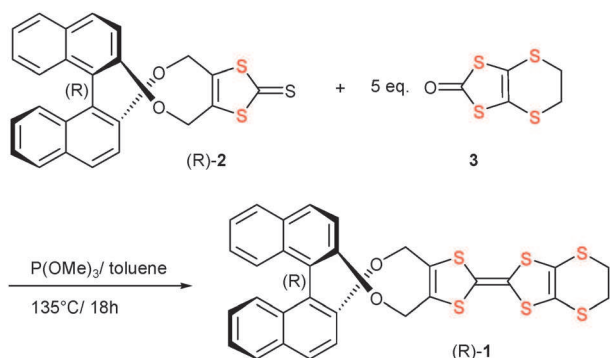
The peculiar geometry adopted by bis(BINOL)TMTTF allowed for an unprecedented self-recognition effect of the (*R,R*) and (*S,S*) enantiomers into mixed-valence dyads, not observed with the *meso* form.¹⁶ However, the strong geometric and steric constraints associated with the presence of *two* binaphthol

moieties did not allow us to isolate any crystalline cation radical salts. Unsymmetrically substituted TTFs bearing only one binaphthol moiety, together with amide or ester functionalities, were also investigated without success for that purpose.¹⁷ We turn here our attention to the unsymmetrically substituted ethylenedithio derivative **1**, since this EDT substitution pattern, present in BEDT-TTF itself but also for example in the chiral (*R*)-MeOXA-EDT-TTF mentioned above,¹¹ appears to strongly favour the crystallisation of cation radical salts, as demonstrated indeed here in the TCNQF₄ salts, we have isolated in a crystalline state with enantiopure (*R*)-**1** and (*S*)-**1**, affording the very first salts of chiral atropoisomeric TTFs.

Results and discussion

Syntheses

The preparation of unsymmetrically-substituted tetrathiafulvalenes,¹⁸ with different substituents on the dithiole rings, can be performed in two different ways. Route (a) involves a selective cross coupling based on the Wittig^{19,20} or Horner–Wadsworth–Emmons²¹ reaction with dithiolium triphenylphosphonium ylide or dithiole phosphonate as nucleophiles. This selective route affords asymmetrically-substituted TTFs in moderate yields, but in a pure form particularly with the phosphonate precursors.^{22,23} Route (b) is based on the statistical cross coupling reaction of two dithiole halves, either dithiolium cations in the presence of NEt₃, or dithiole-2-one or dithiole-2-thione derivatives in the presence of phosphites. This route provides a mixture—to be separated—of three possible TTFs, the two symmetrical ones and the desired unsymmetrical donor molecule. The donor **1** was prepared following this statistical route (b) starting from the chiral 1,3-dithiole-2-thione **2** which is itself prepared from binaphthol and 4,5-bis(bromomethyl)-1,3-dithiole-2-thione.¹⁶ An excess of the 1,3-dithiole-2-one **3** (5 equiv.) was used to favour the formation of the unsymmetrical TTF **1** (Scheme 1). The less soluble symmetrical BEDT-TTF was separated by filtration and the unsymmetrical TTF **1** purified by chromatography and isolated after recrystallisation in 35–45% yield, for the two pure (*R*)-**1** and (*S*)-**1** enantiomers as well as for the racemic mixture (*R,S*)-**1**, starting from (*R*)-**2**, (*S*)-**2** or (*R,S*)-**2** respectively. The purity of the two enantiomers was also assessed from the circular dichroism spectra (Fig. 1). Redox potentials determined by cyclic voltammetry experiments are given in Table 1,



Scheme 1 Preparation of (*R*)-**1**.

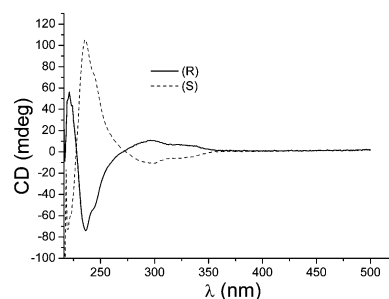


Fig. 1 CD spectra of (*R*)-**1** and (*S*)-**1** in solution in CH₂Cl₂ at 5 × 10^{−5} M.

Table 1 Electrochemical data (in V vs. SCE, CH₂Cl₂, *n*Bu₄PF₆ 0.2 M, scan rate 100 mV s^{−1})

Compound	<i>E</i> _{1/2} ¹	<i>E</i> _{1/2} ²	Reference
Bis(BINOL)TMTTF	0.42	0.97	16
(<i>R,S</i>)- 1	0.484	0.955	This work
(<i>R</i>)- 1	0.487	0.955	This work
(<i>S</i>)- 1	0.488	0.955	This work
EDT-TTF	0.44	0.75	24
BEDT-TTF	0.56	0.80	24

together with reference compounds. The enantiomers and racemic compounds behave similarly, with two reversible redox processes usually observed with TTFs, with the first oxidation potential around 0.49 V vs. SCE.

Molecular and solid state structures

X-Ray crystal structures were obtained for the neutral donor molecule **1**, as racemic mixture (*R,S*)-**1** as well as with the (*R*) enantiomer in a solvate formulated as [(*R*)-**1**]₂·CH₃CN. Racemic (*R,S*)-**1** crystallises in the monoclinic system, space group *P*2₁/*c* with one molecule in general position in the unit cell (Fig. 2). As already observed in the structure of the symmetrical bis(BINOL)TMTTF¹⁶ and other ester or amide derivatives,¹⁷ the ten-membered constrained ring incorporating the binaphthol moiety gives the molecule a very special geometry, with one naphthyl ring perpendicular to the TTF plane.

As shown in Fig. 2, the molecules are associated into inversion-centred dyads, further stabilized with a remarkably short C–H...O interaction. Indeed, while the –CH₂CH₂–ethylene bridge present in EDT-TTF or BEDT-TTF molecules is often disordered on several conformations, it appears here fully fixed in a precise geometry which allows for a defined C–H...O hydrogen bond with the following characteristics, a H...O distance at 2.58 Å, C...O distance at 3.550(3) Å

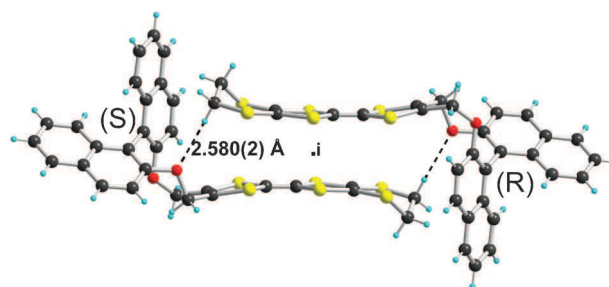


Fig. 2 View of the inversion-centred dyad in neutral (*R,S*)-**1**.

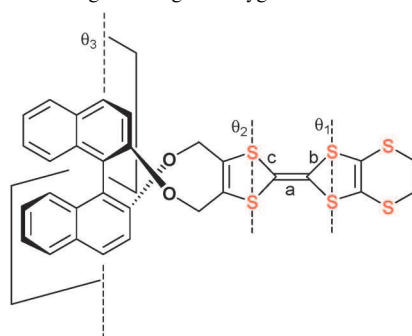
and C–H...O angle at 177°. Intramolecular bond distances and angles are collected in Table 2. Note that within the dyads, the six sulfur atoms of each molecule essentially face each other, but the shortest S...S intermolecular distances exceed 4.16 Å, above twice the sulfur van der Waals radius. In the solid state, the racemic dyads organise into chains running along *b*, as shown in Fig. 3a.

The enantiopure (*R*)-**1** crystallises in the triclinic system, space group *P*1, with two crystallographically independent

molecules in the unit cell, together with one CH₃CN molecule, hence the formulation [(*R*)-**1**]₂·CH₃CN. Intramolecular bond distances and angles (Table 2) are comparable with those described for the racemic mixture. In the solid state (Fig. 3b), the molecules organise into homo-chiral chains of head-to-tail molecules.

The similarity of both structures shown in Fig. 3a and b, for (*R*)-**1** and racemic (*R,S*)-**1**, is only apparent. Indeed, as illustrated in Scheme 2a, the solid state association of the two

Table 2 Bond distances and folding angles in **1** in its various structures. θ_1 and θ_2 are the folding angles of the dithiole ring along the S–S hinge while θ_3 is the dihedral angle between the two benzene rings bearing the oxygen atoms of the binaphthyl moiety



Compound		<i>a</i> /Å	<i>b</i> /Å	<i>c</i> /Å	θ_1 /°	θ_2 /°	θ_3 /°
(<i>R,S</i>)- 1		1.341(4)	1.761(3)	1.765(3)	4.0(1)	11.0(1)	63.46(8)
(<i>R</i>)- 1	Mol. A	1.34(1)	1.762(3)	1.764(3)	14.1(5)	1.2(5)	71.1(2)
			1.716(10)	1.775(8)			
Mol. B		1.35(1)	1.774(9)	1.764(10)	14.9(5)	4.5(5)	64.2(3)
			1.719(9)	1.753(10)			
[(<i>R</i>)- 1] ⁺ •	Mol. A	1.391(7)	1.715(5)	1.730(6)	5.9(3)	2.1(3)	65.0(2)
			1.715(6)	1.725(5)			
Mol. B		1.412(7)	1.712(6)	1.713(5)	3.5(3)	4.1(3)	67.2(2)
			1.716(5)	1.723(6)			
[(<i>S</i>)- 1] ⁺ •	Mol. A	1.396(5)	1.716(4)	1.726(4)	5.8(2)	4.2(2)	65.2(2)
			1.717(4)	1.734(4)			
Mol. B		1.404(5)	1.723(4)	1.717(4)	1.3(2)	3.9(2)	67.6(1)
			1.718(4)	1.729(4)			

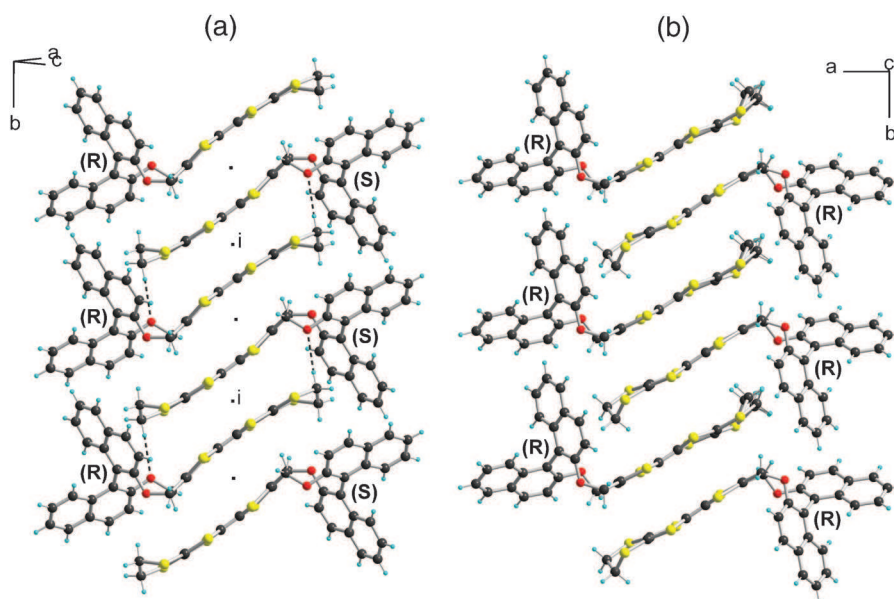
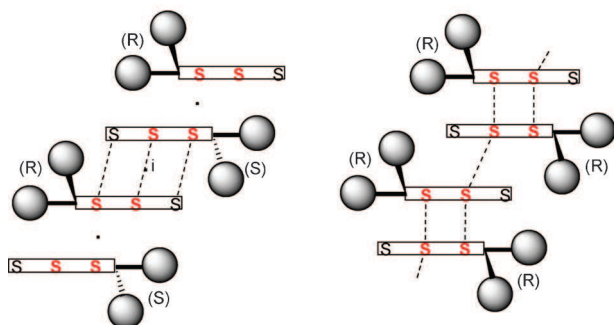


Fig. 3 The solid state organisation of **1**: (a) in the racemic mixture, (b) as (*R*) enantiomer.

(a) in the racemic (*R,S*)-**1** (b) in the enantiopure (*R*)-**1**

Scheme 2 Schematic organisation of the molecules in (*R,S*)-**1** and (*R*)-**1**. The sulfur atoms of the TTF core are highlighted in red, the naphthyl rings are represented by grey balls, the shortest S...S intermolecular contacts with dotted lines.

enantiomers in (*R,S*)-**1** is based on (i) inversion-centred dyads stabilised with the C–H...O hydrogen bonds (Fig. 2) and (ii) a maximum number of sulfur atoms facing each other with long S...S van der Waals interactions within these dyads. In the enantiopure compound (Scheme 2b) on the other hand, shorter S...S van der Waals interactions (3.85 Å and above) take place within homochiral dyads where only the four sulfur atoms of the central TTF moiety are now facing each other. These two structures also demonstrate that molecule **1** is, already in the neutral state, able to associate in the solid state into stacks, a prerequisite for the formation of mixed-valence salts.

Charge-transfer salts

The oxidation potential of **1** (0.49 V vs. SCE) can be compared with the reduction potential of TCNQ (0.17 V) or TCNQF₄ (0.53 V) indicating that the latter acceptor molecule is able to oxidise **1**, while the former is not. Reaction of the three compounds (*R*)-**1**, (*S*)-**1** and (*R,S*)-**1** with TCNQF₄ was performed by diffusion. Crystals could be obtained only with the two enantiomers while the racemic mixture invariably gave very soluble salts which could not be properly crystallised. The two enantiomeric salts crystallise in the triclinic system, space group *P*1, as CH₂Cl₂ solvate. The (*R*) enantiomer will be discussed in the following. It crystallises with two

crystallographically independent [(*R*)-**1**][TCNQF₄].CH₂Cl₂ entities in the unit cell. A projection view of the unit cell of [(*R*)-**1**][TCNQF₄].CH₂Cl₂ along *a* shows that the (*R*)-**1** and TCNQF₄ molecules form segregated stacks and adopt a chessboard organisation reminiscent of that observed in the prototypical TTF·TCNQ charge transfer salt (Fig. 4).

Before investigating in detail the supramolecular solid state characteristics of the compound, we shall first determine the exact redox state of the two components, as the reduction potential of TCNQF₄ is only slightly superior (by 0.05 V) to the oxidation potential of (*R*)-**1** or (*S*)-**1** (see above). As reported in Table 2, a notable lengthening of the central C=C with associated shortening of the internal C–S bond (noted b and c) is observed when going from the neutral (*R*)-**1** to its TCNQF₄ salt, indicating that a charge transfer has indeed occurred. The same geometrical features are found with (*S*)-**1**. The geometrical evolutions within TCNQF₄ (Table 3) also clearly indicate that the latter is in the radical anion form, in both crystallographically independent molecules. This is further substantiated by the $\nu_{C\equiv N}$ vibration observed at 2178 and 2192 cm^{−1} in both [(*R*)-**1**][TCNQF₄].CH₂Cl₂ and [(*S*)-**1**][TCNQF₄].CH₂Cl₂, in accordance with earlier reports for the radical anion species.^{26,27} Therefore, the salts can be confidently formulated as [(*R*)-**1**⁺][TCNQF₄^{−•}].CH₂Cl₂ and [(*S*)-**1**⁺][TCNQF₄^{−•}].CH₂Cl₂, that is, with a full charge transfer.

The solid state organisation of the radical molecules within the stacks is shown in Fig. 5. An interesting comparison can be made with the structure of the chains identified in the neutral donor molecules in (*R*)-**1**, since, as shown in Scheme 3, they are closely related, reflecting the robustness of the stacking organization of the donor molecules. We note that the chains of, respectively, radical cations and radical anions are not uniform as in TTF–TCNQ but strongly dimerised. Overlap interactions (Fig. 6) correspond to an essentially eclipsed conformation for TTF dyads, with very short intra-dyad S...S intermolecular contacts at 3.353(3), 3.452(3), 3.346(3) and 3.428(3) Å while the inter-dyad ones exceed 3.8 Å. A bond-over-ring conformation is observed for the TCNQF₄ dyads. Both overlap geometries are well known to lead to a strong antiferromagnetic pairing of the radical species in the bonding combination of the HOMO of the TTFs and

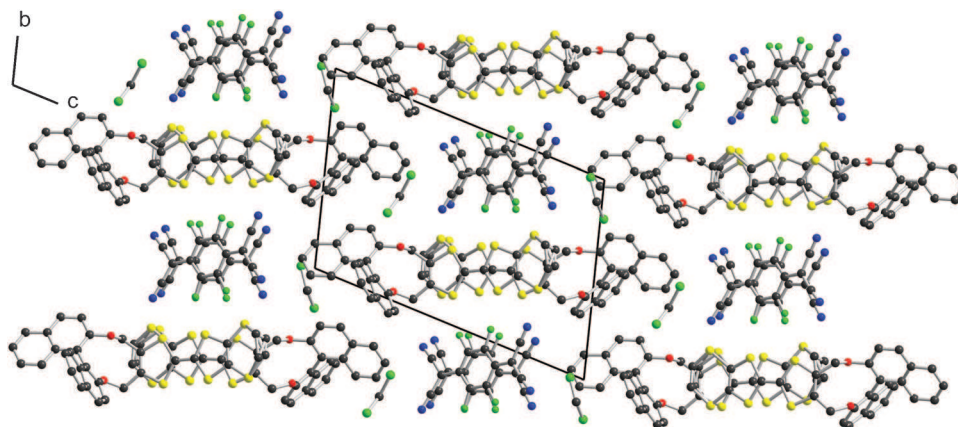
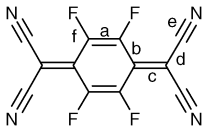
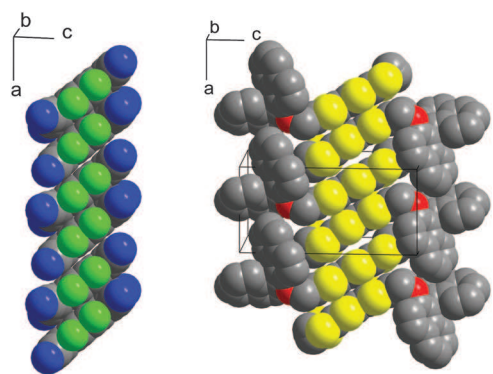
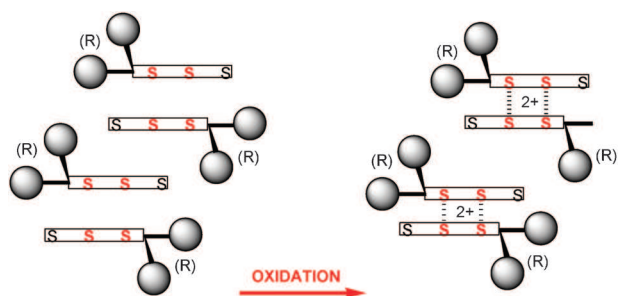
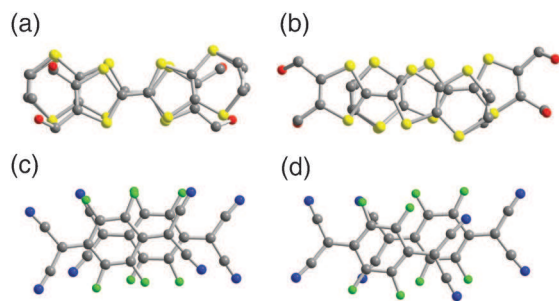


Fig. 4 Projection view along the stacking axis *a* of [(*R*)-**1**][TCNQF₄].CH₂Cl₂.

Table 3 Intramolecular bond distances within TCNQF₄ in various compounds


		<i>a</i> /Å	<i>b</i> /Å	<i>c</i> /Å	<i>d</i> /Å	<i>e</i> /Å	<i>f</i> /Å	Ref.
TCNQF ₄ ⁰		1.334	1.437	1.372	1.437	1.140	1.336	24
TCNQF ₄ with (<i>R</i>)- 1	Mol. 1	1.369(7)	1.417(7)	1.423(7)	1.423(7)	1.143(7)	1.345(7)	This work
	Mol. 2	1.373(7)	1.415(7)	1.412(7)	1.425(7)	1.149(7)	1.342(7)	
TCNQF ₄ ^{•−a}		1.360	1.420	1.429	1.435	1.140	1.349	25
TCNQF ₄ ^{2−a}		1.373	1.398	1.457	1.403	1.154	1.359	26

^a As ferricinium salt.

**Fig. 5** Side view of the stacks of TCNQF₄^{•−} (left) and (**1**)^{•+} (right) running along *a*, showing the strongly dimerised character of the chains.**Scheme 3** Evolution of the donor stacks within the structures of (left) the neutral donor molecules, (right) the oxidised molecules in the TCNQF₄ salt.**Fig. 6** Stronger (a, c) and weaker (b, d) overlap interactions within the association of the (**1**)^{•+} and (TCNQF₄)^{•−} radical species into the stacks. Binaphthyl moieties and hydrogen atoms have been omitted for clarity.

the LUMO of the TCNQF₄ respectively. This analysis is confirmed by the temperature dependence of the magnetic susceptibility for both salts, which exhibit a very weak paramagnetism with a Curie-type behaviour attributable to 1.5% paramagnetic defects (Curie tail) and an insulating behaviour.

Conclusions

We have prepared and structurally characterised a novel chiral TTF derivative, in its racemic and enantiopure forms, based on the atropoisomers of a binaphthol moiety. Despite the strong steric requirements of the bulky binaphthol moiety, both racemic and enantiopure donor molecules are able to organise into stacks in the solid state. The oxidation of the two (*R*) and (*S*) enantiomers with TCNQF₄ allowed for the isolation of 1 : 1 enantiopure salts with the formation of segregated columns of donor and acceptor moieties, both in their radical state. Strong dimerisation within the chains leads here to a singlet ground state. This very first result demonstrates that despite the steric hindrance of the binaphthol moiety, the chiral donor molecule **1** is able to oxidise to cation radical salts with formation of stacks in the solid state. Counter ions other than TCNQF₄^{•−} are being investigated now, particularly by electrocrystallisation with a variety of counter ions.

Experimental

Syntheses

The 1,3-dithiole-2-thiones (*R*)-**2**, (*S*)-**2** and (*R,S*)-**2** were prepared as previously described from the reaction of the corresponding commercially available binaphthol derivatives, as (*R*), (*S*) or racemic mixture, with 4,5-bis(bromomethyl)-1,3-dithiole-2-thione.²⁸ The dithiole-2-one²⁹ **3** and the acceptor³⁰ TCNQF₄ were prepared as previously reported.

(*R,S*)-**1**

A solution of the racemic dithiole-2-thione (*R,S*)-**2** (0.4 g, 0.89 mmol) and the dithiole-2-one **3** (0.96 g, 5 equiv., 4.6 mmol) in freshly distilled P(OMe)₃ (50 mL) is warmed to 130 °C overnight under Ar. After cooling to room temperature, the precipitate (essentially BEDT-TTF) is filtered and washed with CH₂Cl₂. The filtrates are concentrated and purified by chromatography over silica gel (CH₂Cl₂/petrol ether 1/1). Recrystallisation from CH₂Cl₂/ethanol affords (*R,S*)-**1** as

orange crystals (180 mg, 34%). Mp: 210–212 °C. ^1H NMR (300 MHz, CDCl_3) δ 7.89 (d, J = 8.9 Hz, 2H), 7.80 (d, J = 8.1 Hz, 2H), 7.37–7.24 (m, J = 9.4, 8.1, 5.2 Hz, 4H), 7.20–7.04 (m, 4H), 4.91–4.58 (m, 4H), 3.16 (s, 4H). ^{13}C NMR (75 MHz, CDCl_3) δ 153.94, 133.63, 130.25, 129.82, 128.16, 126.61, 126.06, 124.43, 122.30, 117.46, 30.20. Elem. Anal.: Calcd for $(\text{C}_{30}\text{H}_{20}\text{O}_2\text{S}_6)_2(\text{CH}_2\text{Cl}_2)$ (MW = 1294.67): C, 56.59; H, 3.27. Found: C, 56.46; H, 2.85%. Crystals suitable for X-ray diffraction were obtained from CH_3CN .

(R)-1

A solution of the enantiopure dithiole-2-thione (*R*)-2 (0.22 g, 0.49 mmol) and the dithiole-2-one **3** (0.5 g, 5 equiv., 2.39 mmol) in freshly distilled $\text{P}(\text{OMe})_3$ (10 mL) is warmed to 130 °C overnight under Ar. Treatment as above and recrystallisation from CH_2Cl_2 /ethanol affords (*R*)-1 as yellow crystals (120 mg, 42%). Mp: 198 °C. $[\alpha]_{\text{D}}^{20} = +300$. ^1H NMR (300 MHz, CDCl_3) δ 7.89 (d, J = 8.9 Hz, 2H), 7.80 (d, J = 8.1 Hz, 2H), 7.37–7.24 (m, 4H), 7.20–7.05 (m, 4H), 5.02–4.50 (m, 4H), 3.16 (s, 4H). ^{13}C NMR (75 MHz, CDCl_3) δ 153.94, 133.63, 130.25, 129.82, 128.16, 126.61, 126.06, 124.43, 122.30, 117.46, 30.22. Elem. Anal.: Calcd. for $\text{C}_{30}\text{H}_{20}\text{O}_2\text{S}_6$ (MW = 604.87): C, 59.57; H, 3.33. Found: C, 58.87; H, 3.20%. Crystals suitable for X-ray diffraction were obtained from CH_3CN .

(S)-1

A solution of the enantiopure dithiole-2-thione (*S*)-2 (0.15 g, 0.33 mmol) and the dithiole-2-one **3** (0.36 g, 5 equiv., 1.72 mmol) in freshly distilled $\text{P}(\text{OMe})_3$ (10 mL) is warmed to 130 °C overnight under Ar. Treatment as above affords (*S*)-1 as yellow microcrystals (90 mg, 45%). Mp: 200 °C. $[\alpha]_{\text{D}}^{20} = -290$. ^1H NMR (300 MHz, CDCl_3) δ 7.89 (d, J = 8.9 Hz, 2H), 7.80 (d, J = 8.1 Hz, 2H), 7.37–7.24 (m, J = 9.4, 8.1, 5.2 Hz, 4H),

7.20–7.04 (m, 4H), 4.91–4.58 (m, 4H), 3.16 (s, 4H). ^{13}C NMR (75 MHz, CDCl_3) δ 153.94, 133.63, 130.25, 129.81, 128.16, 126.61, 126.06, 124.43, 122.30, 117.46, 30.20. Elem. Anal.: Calcd for $\text{C}_{30}\text{H}_{20}\text{O}_2\text{S}_6$ (MW = 604.87): C, 59.57; H, 3.33. Found: C, 59.40; H, 3.27%.

Charge transfer salts [(*R*)-1]·TCNQF₄·CH₂Cl₂

A solution of the donor (*R*)-1 (5 mg, 1 equiv., 0.0082 mmol) in CH_2Cl_2 (3 mL) in a U tube is layered with a solution of TCNQF₄ (4 mg, 1.7 equiv., 0.0144 mmol) in CH_3CN (3 mL). Black crystals precipitate on the sides and at the bottom of the tube. After four days, the crystals are collected, washed with little CH_2Cl_2 and air-dried (5 mg, 62%). [(*S*)-1]·TCNQF₄·CH₂Cl₂ was obtained in the same way from (*S*)-1.

X-Ray diffraction studies

Single crystals were mounted on the top of a thin glass fiber. Data were collected on a Nonius KappaCCD Diffractometer at room temperature with graphite-monochromated Mo-K α radiation (λ = 0.71073 Å). Structures were solved by direct methods (SHELXS-97) and refined (SHELXL-97)³¹ by full-matrix least-squares methods, as implemented in the WinGX software package.³² Absorption corrections were applied. Hydrogen atoms were introduced at calculated positions (riding model), included in structure factor calculations, and not refined. Crystallographic data of both salts are summarized in Table 4.

Acknowledgements

The authors acknowledge financial support from ANR (France) under grant no. ANR-08-BLAN-0140-02.

Table 4 Crystallographic data

Compound	(<i>R,S</i>)-1	[(<i>R</i>)-1] ₂ ·CH ₃ CN	[(<i>R</i>)-1][TCNQF ₄]·CH ₂ Cl ₂	[(<i>S</i>)-1][TCNQF ₄]·CH ₂ Cl ₂
Formula	$\text{C}_{30}\text{H}_{20}\text{O}_2\text{S}_6$	$\text{C}_{62}\text{H}_{43}\text{NO}_4\text{S}_{12}$	$\text{C}_{43}\text{H}_{22}\text{Cl}_2\text{F}_4\text{N}_4\text{O}_2\text{S}_6$	$\text{C}_{43}\text{H}_{22}\text{Cl}_2\text{F}_4\text{N}_4\text{O}_2\text{S}_6$
FW (g mol ⁻¹)	604.82	1250.69	965.91	965.91
Crystal color	Orange	Orange	Black	Black
Crystal size/mm	0.34 × 0.15 × 0.12	0.09 × 0.05 × 0.02	0.23 × 0.14 × 0.05	0.2 × 0.15 × 0.05
Crystal system	Monoclinic	Monoclinic	Triclinic	Triclinic
Space group	<i>P</i> 2 ₁ / <i>c</i>	<i>C</i> 2	<i>P</i> 1	<i>P</i> 1
<i>T</i> /K	150(2)	150(2)	150(2)	150(2)
<i>a</i> /Å	16.0832(6)	46.597(4)	8.5380(2)	8.5594(3)
<i>b</i> /Å	9.0468(3)	8.8358(7)	12.9927(3)	13.0019(3)
<i>c</i> /Å	18.4128(6)	13.4499(9)	18.7805(5)	18.8153(5)
α°	90.0	90.0	106.570(1)	106.5560(1)
β°	99.842(2)	93.600(3)	90.837(1)	90.8750(1)
γ°	90.0	90.0	92.743(1)	92.7280(1)
<i>V</i> /Å ³	2639.66(16)	5526.7(7)	1993.68(8)	2003.93(10)
<i>Z</i>	4	4	2	2
<i>D</i> _{calc} /g cm ⁻³	1.522	1.503	1.609	1.601
μ /mm ⁻¹	0.548	0.526	0.542	0.540
Total reffs.	14 697	16 538	26 784	32 054
Absorption correction	Multi-scan	Multi-scan	Multi-scan	Multi-scan
<i>T</i> _{min} , <i>T</i> _{max}	0.906, 0.936	0.969, 0.990	0.913, 0.973	0.907, 0.973
Unique reffs. (<i>R</i> _{int})	5944 (0.0447)	9752 (0.0737)	13 579 (0.0360)	15 364 (0.0344)
Reff (<i>I</i> > 2 σ (<i>I</i>))	4398	5150	11 819	14 332
Refined param.	343	707	1137	1137
<i>R</i> ₁ (<i>I</i> > 2 σ (<i>I</i>))	0.0441	0.0746	0.0576	0.0409
<i>wR</i> ₂ (all data)	0.1401	0.2228	0.1760	0.1325
Flack param.	—	0.11(14)	0.06(7)	0.02(4)
Goodness-of-fit	1.102	1.001	1.052	1.098
Res. Dens./e ⁻ Å ⁻³	0.596, -0.583	0.720, -0.591	0.868, -0.926	0.746, -0.658

References

- (a) E. Coronado and P. Day, *Chem. Rev.*, 2004, **104**, 5419; (b) E. Coronado and J. R. Galan-Mascaros, *J. Mater. Chem.*, 2005, **15**, 66.
- N. Avarvari and J. Wallis, *J. Mater. Chem.*, 2009, **19**, 4061 and references therein.
- D. B. Amabilino and J. Veciana, *Top. Curr. Chem.*, 2006, **265**, 253.
- (a) V. Krstic, S. Roth, M. Burghard, K. Kern and G. L. J. A. Rikken, *J. Chem. Phys.*, 2002, **117**, 11315; (b) V. Krstic and G. L. J. A. Rikken, *Chem. Phys. Lett.*, 2002, **364**, 51.
- (a) E. Coronado, J. R. Galan-Mascaros, C. J. Gomez-Garcia, A. Murcia-Martinez and E. Canadell, *Inorg. Chem.*, 2004, **43**, 8072; (b) J. R. Galan-Mascaros, E. Coronado, P. A. Goddard, J. Singleton, A. I. Coldea, J. D. Wallis, S. J. Coles and A. Alberola, *J. Am. Chem. Soc.*, 2010, **132**, 9271.
- M. Brezgunova, K.-S. Shin, O. Jeannin, P. Auban-Senzier and M. Fourmigué, *Chem. Commun.*, 2010, **46**, 3226.
- L. Martin, P. Day, P. Horton, S. Nakatsuji, J. Yamada and H. Akutsu, *J. Mater. Chem.*, 2010, **20**, 2738.
- J. D. Wallis, A. Karrer and J. D. Dunitz, *Helv. Chim. Acta*, 1986, **69**, 69.
- (a) J. D. Wallis and J.-P. Griffiths, *J. Mater. Chem.*, 2005, **15**, 347; (b) J.-P. Griffiths, H. Nie, R. J. Brown, P. Day and J. D. Wallis, *Org. Biomol. Chem.*, 2005, **3**, 2155; (c) S. Yang, A. C. Brooks, L. Martin, P. Day, H. Li, L. Male, P. Horton and J. D. Wallis, *CrystEngComm*, 2009, **11**, 993.
- S. Kimura, T. Maejima, H. Suzuki, R. Chiba, H. Mori, T. Kawamoto, T. Mori, H. Moriyama, Y. Nishio and K. Kajita, *Chem. Commun.*, 2004, 2454.
- C. Réthoré, N. Avarvari, E. Canadell, P. Auban-Senzier and M. Fourmigué, *J. Am. Chem. Soc.*, 2005, **127**, 5748–5749.
- (a) C. Réthoré, A. Madalan, M. Fourmigué, E. Canadell, E. Lopes, M. Almeida, R. Clérac and N. Avarvari, *New J. Chem.*, 2007, **31**, 1468; (b) A. M. Madalan, C. Réthoré, M. Fourmigué, E. Canadell, E. B. Lopes, M. Almeida, P. Auban-Senzier and N. Avarvari, *Chem.–Eur. J.*, 2010, **16**, 528.
- (a) J. S. Zambounis, C. W. Mayer, K. Hauenstein, B. Hilti, W. Hofherr, J. Pfeiffer, M. Bürkle and G. Rihs, *Adv. Mater.*, 1992, **4**, 33; (b) J. S. Zambounis, J. Pfeiffer, G. C. Papavassiliou, D. J. Lagourvados, A. Terzis, C. P. Raptopoulou, P. Delhaes, L. Ducasse, N. A. Fortune and K. Murata, *Solid State Commun.*, 1995, **95**, 211; (c) J. D. Wallis and J. D. Dunitz, *Acta Crystallogr., Sect. C: Cryst. Struct. Commun.*, 1988, **44**, 1037.
- R. Gomez, J. L. Segura and N. Martin, *J. Org. Chem.*, 2000, **65**, 7566.
- (a) Y. Zhou, D. Zhang, L. Zhu, Z. Shuai and D. Zhu, *J. Org. Chem.*, 2006, **71**, 2123–2130; (b) H. Wu, D. Zhang and D. Zhu, *Tetrahedron Lett.*, 2007, **48**, 8951.
- A. Saad, F. Barrière, E. Levillain, N. Vanthuyne, O. Jeannin and M. Fourmigué, *Chem.–Eur. J.*, 2010, **16**, 8020.
- A. Saad, O. Jeannin and M. Fourmigué, *CrystEngComm*, 2010, **12**, 3866.
- J.-M. Fabre, *Chem. Rev.*, 2004, **104**, 5133.
- C. Gonnella and M. P. Cava, *J. Org. Chem.*, 1978, **43**, 369.
- (a) J.-M. Fabre, C. Galaine, L. Giral and D. Chasseau, *Tetrahedron Lett.*, 1982, **23**, 1813; (b) L. Giral, J.-M. Fabre and A. Gouasmia, *Tetrahedron Lett.*, 1986, **27**, 4315; (c) J.-M. Fabre, L. Giral, A. Gouasmia, H.-J. Cristau and Y. Ribeill, *Bull. Soc. Chim. Fr.*, 1987, **5**, 823.
- K. Lerstrup, I. Johannsen and M. Jorgensen, *Synth. Met.*, 1988, **27**, B9.
- (a) M. Fourmigué and P. Batail, *Bull. Soc. Chim. Fr.*, 1992, **129**, 29; (b) M. Fourmigué and Y.-S. Huang, *Organometallics*, 1993, **12**, 797; (c) M. Fourmigué, F. C. Krebs and J. Larsen, *Synthesis*, 1993, 509; (d) F. Gerson, A. Lamprecht and M. Fourmigué, *J. Chem. Soc., Perkin Trans. 1*, 1996, 1409; (e) M. Fourmigué, C. Mézière, E. Canadell, D. Zitoun, K. Bechgaard and P. Auban-Senzier, *Adv. Mater.*, 1999, **11**, 766.
- M. Fourmigué, E. W. Reinheimer, K. R. Dunbar, P. Auban-Senzier, C. Pasquier and C. Coulon, *Dalton Trans.*, 2008, 4652.
- V. Khodorkovsky, A. Edzifina and O. Neilands, *J. Mol. Electron.*, 1989, **5**, 33.
- T. J. Emge, M. Maxfield, D. O. Cowan and T. J. Kistenmacher, *Mol. Cryst. Liq. Cryst.*, 1981, **65**, 161.
- J. S. Miller, J. H. Zhang and W. M. Reiff, *Inorg. Chem.*, 1987, **26**, 600.
- D. A. Dixon, J. C. Calabrese and J. S. Miller, *J. Phys. Chem.*, 1989, **93**, 2284.
- P. Hudhomme, S. Le Moustarder, C. Durand, N. Gallego-Planas, N. Mercier, P. Blanchard, E. Levillain, M. Allain, A. Gorgues and A. Riou, *Chem.–Eur. J.*, 2001, **7**, 5070.
- J. Larsen and C. Lenoir, *Synthesis*, 1989, 134.
- R. C. Wheland and E. L. Martin, *J. Org. Chem.*, 1975, **40**, 3101.
- SHELX97-Programs for CrystalStructure Analysis (Release 97-2). G. M. Sheldrick (1998).
- L. J. Farrugia, *J. Appl. Crystallogr.*, 1999, **32**, 837.